

SLAC-PUB-7711

November 1997

## **Electron-Electron Luminosity in the Next Linear Collider—A Preliminary Study\***

F. Zimmermann, K.A. Thompson and R.H. Helm

Stanford Linear Accelerator Center, Stanford University, California 94309

In this paper, we discuss some operational aspects of electron-electron collisions at the Next Linear Collider (NLC) and estimate the luminosity attainable in such a machine. We also consider the use of two future technologies which could simplify the operation and improve the luminosity in an  $e^-e^-$  collider: polarized rf guns and plasma lenses.

*Invited Talk at the Second International Workshop on Electron-Electron Interactions at TeV Energies  
Santa Cruz, California, September 22-24, 1997*

---

\*Work supported by the U.S. Department of Energy under the Contract No. DE-AC03-76SF00515.

# ELECTRON-ELECTRON LUMINOSITY IN THE NEXT LINEAR COLLIDER—A PRELIMINARY STUDY\*

F. ZIMMERMANN, K.A. THOMPSON and R.H. HELM  
*Stanford Linear Accelerator Center, Stanford University, CA 94309*

In this paper, we discuss some operational aspects of electron-electron collisions at the Next Linear Collider (NLC) and estimate the luminosity attainable in such a machine. We also consider the use of two future technologies which could simplify the operation and improve the luminosity in an  $e^-e^-$  collider: polarized rf guns and plasma lenses.

## 1. Introduction

The rich particle physics accessible at the Next Linear Collider (NLC) could be further enhanced when in addition to electron-positron collisions also electron-electron collisions are realized. The strong physics case for an electron-electron collider has been described elsewhere.<sup>1</sup>

In this report, we first discuss the (few) steps required to convert the NLC from an  $e^+e^-$  to an  $e^-e^-$  collider. We then describe how the performance of an  $e^-e^-$  collider could be greatly improved by use of polarized rf guns. Subsequently, we present simulation results for the collision of two flat or round electron beams (assuming the latter might be produced by an rf gun), from which we can estimate the luminosity attainable in an  $e^-e^-$  collider. We compare the luminosity, disruption angles, and energy loss for three different  $e^-e^-$  scenarios with those expected for the nominal flat-beam  $e^+e^-$  parameters. This is followed by a brief discussion on how the luminosity could be improved and, perhaps, the beamstrahlung significantly suppressed with a plasma lens placed at the interaction point. Finally, we will draw some preliminary conclusions.

## 2. Switch from $e^+e^-$ to $e^-e^-$

The NLC design permits a simple switch from  $e^+e^-$  to  $e^-e^-$  operation. Only the following few changes to the accelerator operation would be required:

- bypassing the  $e^+$ -production target and the pre-damping ring; Figure 1 illustrates that this is straightforward;
- reversing the polarity of all downstream magnets (and adjusting those beam diagnostics which are sensitive to the beam charge)

---

\*Work supported by the US Department of Energy under Contract DE-AC03-76SF00515.

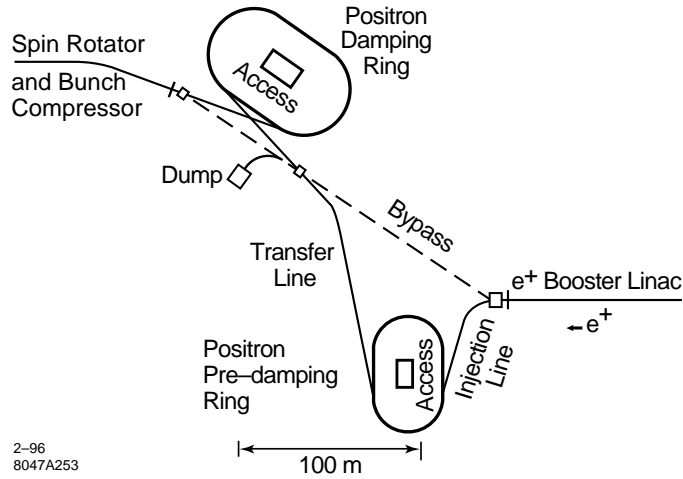


Fig. 1. Layout of the positron damping ring complex along with the two bunch compressors and the positron source, demonstrating that bypass transfer lines suitable for  $e^-e^-$  operation are an inherent part of the NLC design.<sup>2</sup>

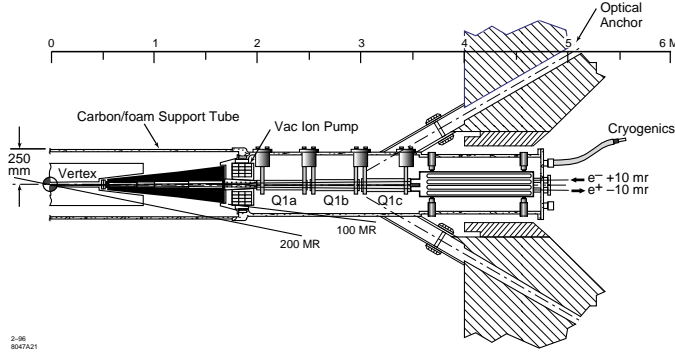


Fig. 2. Schematic of the permanent quadrupole-pair and the superconducting quadrupole pair in the NLC final doublet next to the interaction point for a 20-mr crossing angle.<sup>2</sup>

- replacing the thermionic  $e^-$  gun, that is used to generate the  $e^-$  drive beam for  $e^+$  production, with a polarized gun (the geometrical constraints for spin rotation are already part of the  $e^+$  system design<sup>2</sup>)
- rotating the (permanent) quadrupole closest to the interaction point (see Fig. 2), *or*, if possible, to use a second interaction point with a dedicated  $e^-e^-$  final-focus system

Thanks to the 20-mr crossing angle, the two colliding beams in the NLC are transported through separate beam lines on both sides of the IP. Because the beam lines for the incoming and outgoing beams are completely independent, all magnet power supplies can be reversed and no optics changes from the  $e^+e^-$  mode of operation would be necessary when switching to  $e^-e^-$  collisions<sup>a</sup>. By contrast, the

<sup>a</sup>We assume here that the apertures of the exit quadrupoles and the extraction lines are large

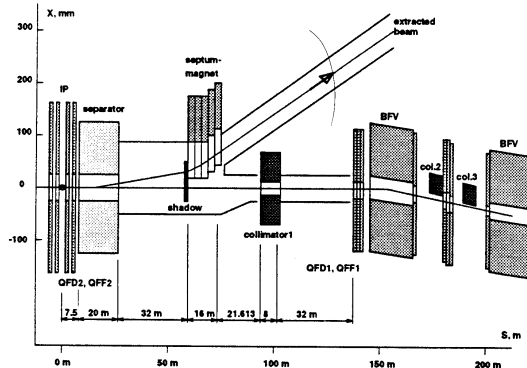


Fig. 3. Layout of the TESLA beam extraction system behind the IP.<sup>3</sup> After the final doublet the exiting beam passes through an electrostatic separator followed by septum magnets.

TESLA design<sup>3</sup> (Fig. 3) contemplates head-on collisions, in which case at least the first few quadrupoles after the IP are common to both beams, and a switch from  $e^+e^-$  to  $e^-e^-$  collisions would necessitate a different beam optics.

### 3. RF Guns and Round Beams

In recent years, substantial progress has been made in the development of polarized photocathodes, best exemplified by the success of the SLAC photoinjector, and also in the design and construction of rf guns. Though considerable difficulties still must be overcome, the possibility of combining these two technologies so as to develop a polarized rf gun is thought to be within reach.<sup>4,5</sup> From the accelerator-physics point of view, such a polarized rf gun would greatly strengthen the case of the  $e^-e^-$  collider.

As an illustration of the potential benefit, let us assume two polarized rf guns producing round beams with normalized emittances of  $\gamma\epsilon_{x,y} \approx 1 \mu\text{m}$  and  $\sim 100 \mu\text{m}$  bunch length become available. Feeding the main linacs directly from such rf guns would offer the following obvious advantages:

- no need for any damping rings or pre-damping rings
- no need for bunch compressors
- no need for an injector complex upstream of damping rings
- much less complexity, resulting in improved performance and increased reliability
- much looser alignment and vibration tolerances (which scale roughly as  $\sim 1/\sqrt{\epsilon_y} \sim 5$ )
- polarization of both beams

---

enough to accommodate the heavily disrupted beams in  $e^-e^-$  collisions.

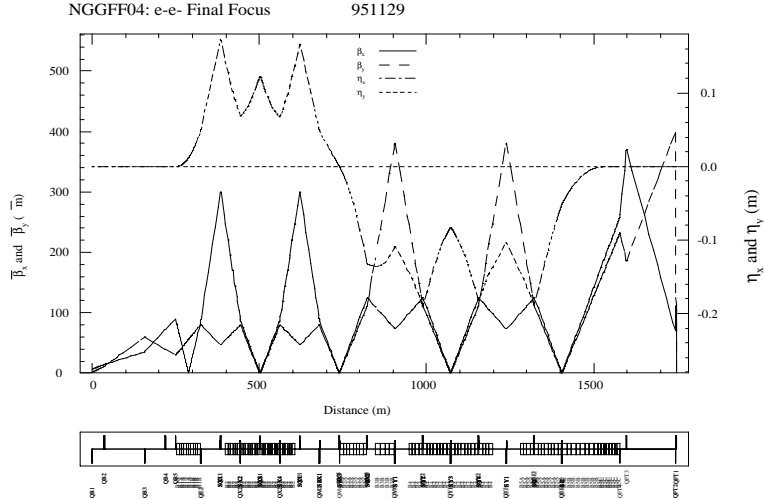


Fig. 4. Final-focus optics with  $\beta_x^* = \beta_y^* = 0.5$  mm.

- the possibility of a higher repetition rate, which would be decoupled from the damping-ring circumference and damping times; this could yield an improved tuning convergence, decreased feedback response times and a higher overall stability.

If both transverse emittances are equal, round-beam collisions are a natural option. Figure 4 shows the optics of a final-focus system with equal horizontal and vertical beta functions,  $\beta_x \approx \beta_y \approx 0.5$  mm at the interaction point, which would be suitable for round-beam  $e^-e^-$  collisions. The system length is almost the same as that for a flat-beam  $e^+e^-$  collider,<sup>2</sup> about 1.8 km. It would increase further if even smaller IP beta functions are desired.

The only drawback of the rf-gun scenario are the disruption effects that occur for round-beam electron-electron collisions. These appear to be quite serious (see discussion in the following section), unless they can be compensated by a plasma at the interaction point. If such a compensation turns out to be impossible or impractical, it still might be possible to realize all the above benefits, without introducing any harmful disruption effects, by a hypothetical *flat-beam polarized rf gun*.

#### 4. Beam-Beam Effects and Luminosity

Table 1 lists a set of nominal NLC interaction-point beam parameters for  $e^+e^-$  operation and an equivalent almost identical set for  $e^-e^-$  collisions. In the bottom part of the table we compare the results of beam-beam simulations performed with the code Guinea-Pig<sup>8</sup> for the above parameters. The table shows that, when compared with the  $e^+e^-$  case, the anti-pinch effect experienced in  $e^-e^-$  collisions causes two major problems:

- an increase of the vertical divergence of the spent beam by a factor of 4–5, which is likely to require additional beam stay-clear in the extraction line, and

mode	$e^+e^-$ flat	$e^-e^-$ flat	comment
$E$ [TeV]	1		c.m. energy
$\gamma\epsilon_x$ [ $\mu\text{m rad}$ ]	4		norm. hor. emittance
$\gamma\epsilon_y$ [ $\mu\text{m rad}$ ]	0.09		norm. vert. emittance
$\sigma_x$ [mm]	200		hor. spot size
$\sigma_y$ [mm]	3.35		vert. spot size
$\beta_x^*$ [mm]	10		hor. IP beta function
$\beta_y^*$ [mm]	0.125		vert. IP beta function
$\sigma_z$ [ $\mu\text{m}$ ]	125		bunch length
$D_x$	0.16		hor. discr. param.
$D_y$	9.8		vert. discr. param.
$N_b$ [ $10^{10}$ ]	0.95		# particles per bunch
$n_b$	90		# bunches
$f$	180		# bunch trains per s
$\theta_x$ [ $\mu\text{rad}$ ]	164	145	hor. div. of spent beam
$\theta_y$ [ $\mu\text{rad}$ ]	35	145	vert. div. of spent beam
$H_D$	1.25	0.40	enhancement factor
$N_\gamma$	1.8	1.6	no. of photons/electron
$\langle dE/E \rangle$ [%]	11.3	10.6	av. energy loss
$\langle dE/E \rangle_{\text{rms}}$ [%]	14	14	rms energy spread
$L$ [ $10^{34} \text{ cm}^{-2} \text{ s}^{-1}$ ]	1.16	1.16	luminosity w/o disruption
$L$ [ $10^{34} \text{ cm}^{-2} \text{ s}^{-1}$ ]	1.45	0.46	luminosity w. disruption

Table 1. Parameters for  $e^+e^-$  (nominal NLC parameters NLC-IIa<sup>2</sup>) and  $e^-e^-$  collisions with flat beams, as obtained from beam-beam simulations with Guinea-Pig.<sup>8</sup>

- a factor of 3 loss in luminosity as compared with the electron-positron case.

One possible remedy is to build a dedicated IP and final-focus system for  $e^-e^-$  collisions, which would be optimized for the modified parameters of the spent beam. Another is to use a plasma lens to increase the luminosity and to reduce the disruption of the electron beams at the IP.

Assuming that two polarized rf guns with the above parameters are in place, we have also studied the round-beam collisions and the expected round-beam luminosity. For illustration purposes, we have considered two different values of the IP beta functions, both not too far from the example optics of Fig. 4. These beam parameters and the results of beam-beam simulations with the code Guinea-Pig<sup>8</sup> are listed in Table 2. The vertical and horizontal angular divergences of the spent beam are dramatically increased, by a factor of 4–5 compared with the flat-beam  $e^-e^-$  collisions, and by an even larger factor of 20 compared with the nominal  $e^+e^-$  case (see Table 1).

Figure 5 shows the luminosity spectra (luminosity per energy interval) for the different electron-positron and electron-electron collision modes considered in this paper. The average energy loss and final energy spread as well as the number of photons emitted per electron for each case were listed in Tables 1 and 2. Using the formula<sup>9</sup>

$$\frac{\Delta L}{L_0} = \frac{1}{N_\gamma^2} [1 - e^{-N_\gamma}]^2 \quad (1)$$

	$e^-e^-$ round (a)	$e^-e^-$ round (b)	comment
$E$ [TeV]	1	1	c.m. energy
$\gamma\epsilon_x$ [ $\mu\text{m rad}$ ]	1	1	norm. hor. emittance
$\gamma\epsilon_y$ [ $\mu\text{m rad}$ ]	1	1	norm. vert. emittance
$\sigma_x$ [nm]	26	16	hor. spot size
$\sigma_y$ [nm]	26	16	vert. spot size
$\beta_x^*$ [mm]	0.68	0.25	hor. IP beta function
$\beta_y^*$ [mm]	0.68	0.25	vert. IP beta function
$\sigma_z$ [ $\mu\text{m}$ ]	125	125	bunch length
$D_x$	4.9	13.0	hor. disr. param.
$D_y$	4.9	13.0	vert. disr. param.
$N_b$ [ $10^{10}$ ]	0.95	0.95	# particles per bunch
$n_b$	90	90	# bunches
$f$	180	180	# bunch trains per s
$\theta_x$ [ $\mu\text{rad}$ ]	491	564	hor. div. of spent beam
$\theta_y$ [ $\mu\text{rad}$ ]	574	764	vert. div. of spent beam
$H_D$	0.40	0.24	enhancement factor
$N_\gamma$	3.8	4.4	no. of photons/electron
$\langle dE/E \rangle$ [%]	36.5	45	av. energy loss
$\langle dE/E \rangle_{\text{rms}}$ [%]	26	27	rms energy spread
$L$ [ $10^{34} \text{ cm}^{-2} \text{ s}^{-1}$ ]	1.16	3.55	luminosity w/o disruption
$L$ [ $10^{34} \text{ cm}^{-2} \text{ s}^{-1}$ ]	0.46	0.85	luminosity w. disruption

Table 2. Parameters for  $e^-e^-$  collisions with round beams produced by a hypothetical (polarized) rf gun, as obtained from beam-beam simulations with Guinea-Fig.<sup>8</sup>

for the fraction of the luminosity at the full nominal energy, we find that this fraction equals 25% for flat beam  $e^-e^-$  collisions and only 5% for the (unneutralized) round-beam collisions. Both the very high divergence angles as well as the very small fraction of luminosity at nominal energy clearly disfavor the pure round-beam collisions without plasma neutralization (plasma lenses are discussed in the next section).

In Fig. 6, we show, as a function of the vertical offset between the two colliding beams, the luminosity enhancement factor  $H_D$ , *i.e.*, the luminosity increase or decrease compared to the geometrical luminosity that would be expected for the head-on collision of two rigid Gaussian bunches. The anti-pinch effect for an electron-electron collider is reflected both in the luminosity reduction for head-on collisions and in the increased sensitivity to relative vertical offsets  $\Delta y$ .

At the Stanford Linear Collider, a standard means to maintain collisions and to measure the convoluted beam sizes at the interaction point is to perform beam-beam deflection scans, where the deflection angle of either beam is measured as a function of the transverse displacement of the two beams, which is varied using fast steering correctors.

The shape of the beam-beam deflection scans in an  $e^-e^-$  collider will be different from that in an  $e^+e^-$  collider, because in the former case the two beams repel each other. A comparison of a vertical deflection scan for  $e^+e^-$  and  $e^-e^-$  collisions is shown in Fig. 7, which also includes the theoretical shape for undisturbed (or

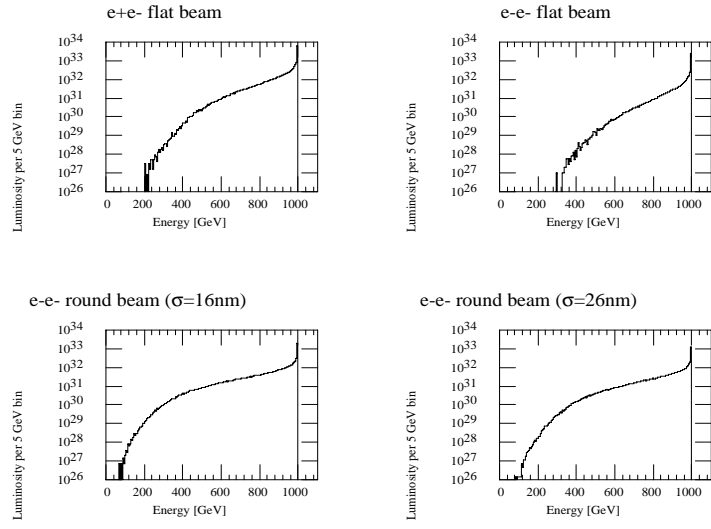


Fig. 5. Luminosity spectra for flat-beam  $e^+e^-$  collisions (upper left), flat-beam  $e^-e^-$  collisions (upper right), and round-beam  $e^-e^-$  collisions (lower left and right).

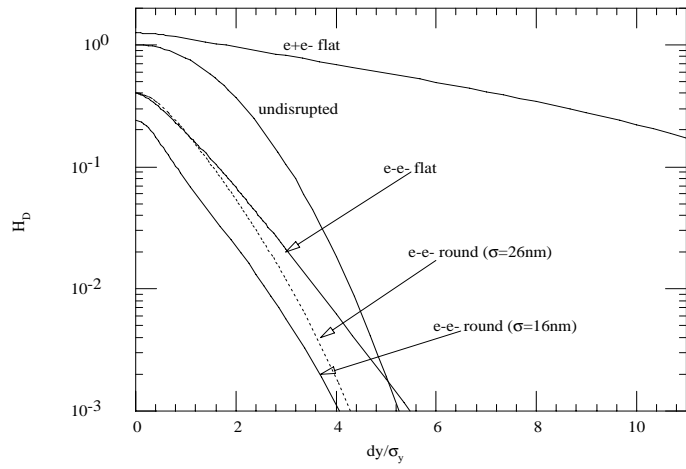


Fig. 6. Luminosity enhancement factor as a function of the vertical displacement of the two beams, for round and flat  $e^+e^-$  and  $e^-e^-$  collisions.



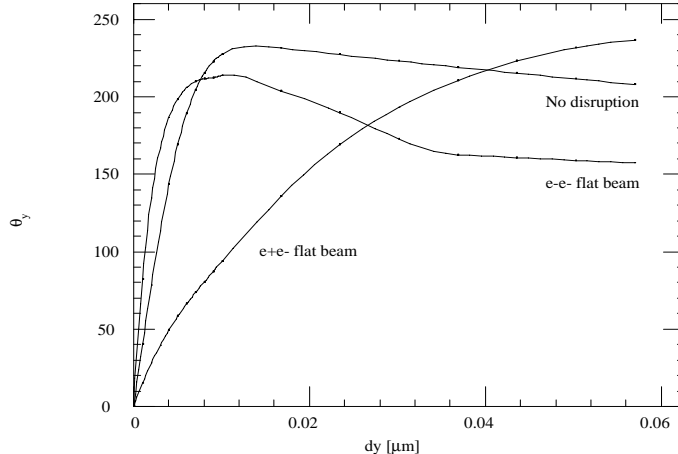


Fig. 7. Absolute value of the vertical deflection angle (in  $\mu\text{rad}$ ) as a function of the relative vertical position of the two beams at the interaction point, comparing flat-beam  $e^+e^-$ ,  $e^-e^-$  and rigid bunch collisions.

low-current) beams. For the  $e^-e^-$  flat-beam NLC parameters, the slope of the vertical scan is about twice that for  $e^+e^-$  collisions. This will allow to measure the beam sizes twice as accurately, and, assuming the deflection angle is zeroed by an interaction-point orbit feedback as utilized in the SLC, it will allow maintaining the collisions with a two times improved precision. Therefore the increased sensitivity to vertical offsets will likely be cancelled by the improved response of the feedback system. As a result the average fractional luminosity loss due to orbit motion will not be very different from the  $e^+e^-$  case.

## 5. Plasma Lenses

### 5.1. Focusing Plasma Lens

If a plasma is placed just in front of the interaction point, the additional focusing of the electron beam by the plasma can lead to a significantly reduced beta function at the IP. This was studied by Chen and others,<sup>6,7</sup> who found that the reduced beta function is given by

$$\frac{\beta_{x,y}^*}{\beta_{0,x,y}^*} = \frac{1}{1 + K\beta_{0,x,y}^*\bar{\beta}_{x,y}} \quad (2)$$

where  $K \approx 2\pi r_e n_p / \gamma$  ( $n_p$  is the plasma density) denotes the quadrupole gradient of the plasma lens,  $\beta_{0,x,y}^*$  the horizontal (vertical) IP beta function without the plasma lens, and  $\bar{\beta}_{x,y}$  the beta function at the entrance of the lens:

$$\bar{\beta}_{x,y} = \beta_{0,x,y}^* \left( 1 + \left( \frac{d}{\beta_{0,x,y}^*} \right)^2 \right) \quad (3)$$

Here  $d$  is the thickness of the plasma lens.

As an example,<sup>6</sup> we consider a lens of thickness  $d = 3$  mm, and with a plasma density of  $n_p \approx 10^{19}$  cm<sup>-3</sup>. Then  $K \approx 18$  cm<sup>-2</sup>, and from Eqs. (2) and (3) we find for the flat-beam case:  $\beta_x^*/\beta_{0,x}^* \approx 0.05$ , and  $\beta_y^*/\beta_{0,y}^* \approx 0.98$ . Overall, this gives about a factor of 4 more luminosity. Similarly for the round-beam  $e^-e^-$  cases, we have  $\beta_{x,y}^*/\beta_{0,x,y}^* \approx 0.4$ , so that we expect a luminosity increase by roughly a factor of 2.5.

A positron beam responds very differently to a plasma lens than an electron beam. Although it is not impossible to also focus a positron beam with a plasma, such focusing will introduce strong optical aberrations.<sup>11</sup> The use of focusing plasma lenses is much more natural for the symmetric collision of two electron beams, where the plasma focusing is nearly aberration free.<sup>11</sup>

## 5.2. Full Neutralization by Interaction-Point Plasma

Since, contrary to an  $e^+e^-$  collider, for  $e^-e^-$  operation there is a net beam charge during the collision process, a suitably dense plasma placed at the interaction point may completely compensate the anti-pinch effect and suppress the beamstrahlung. A full compensation would require a plasma with a density equal to, or larger than, twice the beam density:

$$n_{pl} \geq \frac{2N_e}{(2\pi)^{3/2}\sigma_x\sigma_y\sigma_z} \sim 1.5 \times 10^{22} \text{ cm}^{-3} \quad (4)$$

This is comparable to the density of typical solids. Feasibility and background implications of such a scheme remain to be investigated in detail. The inelastic scattering rate in a plasma was estimated by Chen et al.<sup>11</sup> It should be possible to handle the expected background, *e.g.*, by using detector technology as developed for B physics studies at hadron colliders or for the LHC.

We speculate that the optimum plasma is one which first focuses the two beams and then, during the collision, suppresses the beamstrahlung. If the plasma-density gradient is properly chosen, we may even realize an adiabatic focuser as proposed by Chen, Oide, Sessler and Yu.<sup>10</sup> In this way we would overcome the Oide limit on the vertical spot size.<sup>10</sup> A new limit on the spot size arises from energy-loss considerations, which reads<sup>10</sup>

$$\sigma_q \gg (1.39 \times 10^{-8} \text{ m}) \xi^2 \exp\left(-\frac{1.12}{\xi}\right) \quad (5)$$

where  $\xi = (\gamma\epsilon_y/\epsilon_c)^{1/3}$  and  $\epsilon_c \approx 6.2 \mu\text{m}$  the critical emittance. For a normalized beam emittance of  $\gamma\epsilon \approx 1 \mu\text{m}$ , we find  $\sigma_q \gg 0.52$  nm, which is small compared to our design beam sizes in Tables 1 and 2.

## 6. Conclusions

The design of the NLC permits a fast and easy switch to  $e^-e^-$  operation, which should readily achieve electron-electron luminosities of  $5 \times 10^{33} - 10^{34}$  cm<sup>-2</sup> s<sup>-1</sup>. The enhanced disruption angles might make it more difficult to cleanly extract the

spent beam. This problem could be eased by a dedicated interaction point and extraction line for  $e^-e^-$  collisions.

Two focusing plasma lenses placed close to (and on either side of) the interaction point would enhance the luminosity at least by a factor of 2–4. Larger luminosity increases appear possible with a thicker and/or denser plasma. Even more excitingly, electron-electron collisions might open up the possibility of fully neutralizing the beam charge density during the collision process by means of a high-density plasma, and, thereby, greatly suppressing the beamstrahlung.

Electron-electron collisions would also benefit the most from polarized rf guns. If only round-beam rf guns are available, a plasma-based neutralization scheme at the IP will be necessary in order to ameliorate the very strong disruption effects. A polarized flat-beam rf gun would offer basically the same advantages as a round-beam rf gun, and in addition it would not have to rely on such compensation techniques.

Research on polarized rf guns and studies of anti-pinch compensation schemes conducted today could show a great payoff on the day when the first  $e^-e^-$  linear collider commences operation.

## 7. Acknowledgements

We thank C. Heusch for urging one of us (F.Z.) to give this talk, and P. Chen, R. Siemann, J. Spencer and D. Whittum for helpful discussions.

## References

1. C. Heusch, “Linear Electron-Electron Colliders”, invited talk at the workshop on future high-energy colliders, Santa Barbara October 21–25, 1996, SLAC-PUB-7436 (1997).
2. Zeroth-Order Design Report for the Next Linear Collider, SLAC Report 474, LBNL-PUB-5424, UCRL-ID-124161 (1996).
3. R. Brinkmann, G. Materlik, J. Rossbach, A. Wagner (eds.), et al., “Conceptual Design of a 500 GeV  $e+e-$  Collider with Integrated X-Ray Laser Facility”, DESY 97-048 (1997).
4. J. Clendenin et al., “Prospects for generating polarized electron beams for a linear collider using an rf gun”, Nucl. Instr. Meth. A 340 p. 133 (1994).
5. S. Schreiber, “An RF Gun as a Polarized Source for TESLA”, TESLA 97-01 (1997).
6. P. Chen, A. Spitkovsky and A. Weidemann, “Beam-Beam Disruption and the Case for a Plasma Lens in  $e^-e^-$  Collisions”, Int. Journ. of Mod. Phys. A, Vol. 11, no. 9 p. 1687–1692 (1996).
7. P. Chen, C.K. Ng and S. Rajagopalan, “Luminosity enhancement by a self-ionized plasma in  $e+ / e-$  collisions”, Physical Review E 48, no. 4 (1993).
8. The code Guinea-Pig was written by D. Schulte at DESY (now CERN).
9. P. Chen, “Differential Luminosity under Multiphoton Beamstrahlung”, Phys. Rev. D 46, 1186 (1992).
10. P. Chen, K. Oide, A.M. Sessler, and S.S. Yu, “An adiabatic focuser”, Part. Acc. 31, p.7–19 (1990).
11. P. Chen, S. Rajagopalan, J. Rosenzweig, “Final focusing and enhanced disruption from an underdense plasma lens in a linear collider”, Phys. Rev. D, p. 923 (1989).